J. Geotech, Eng., JSCE, No. 687/III-56, 1-8, 2001 September

UNDRAINED STRAIN SOFTENING BEHAVIOR OF NORMALLY CONSOLIDATED CLAYS AND MUD ROCKS

Michio YAMADA[1], Masaru AKAISHI[2] and Yannis F. DAFALIAS[3]

[1]Member of JSCE, M. Eng., Chief Engineer, Designing Division, Ohba Ltd.
(4-4-12, Aobadai, Meguro-ku, Tokyo 153-0042, Japan)
[2]Member of JSCE, Dr. Eng., Professor , Dept. of Civil Eng. Tokai University
(1117, Kitakaname, Hiratukashi, Kanagawa 259-12, Japan)
[3]Member of ASCE, Ph.D., Professor, Dept. of Civil & Enviromental Eng., University of California, Davis and Division of Mechanics, National Technical University of Athens
(Davis, CA95616-5294, USA and Athens 15773, Hellas)

Elasto-plastic constitutive models for the undrained strain softening behavior of normally consolidated clays and mud rocks are proposed by using the non associated flow rule. Parametric studies are performed on three proposed yield functions to examine the applicability and limitation of the models. The simulated strain softening behavior is compared with the undrained triaxial compression test results for alluvial clay and diatomaceous mud rock. It is concluded that one of the proposed models is appropriate for the simulation of undrained stress strain relations taking account of the strain softening behavior.

Key Words: *strain softening, elasto plastic constitutive model, normally consolidated clay*

1. INTRODUCTION

The maximum shearing strength of soil is generally used when examining the stability of soft ground by the total stress method ($\phi_u = 0$ method), and it is assumed that it develops simultaneously in the whole sliding surface. On the other hand the shearing stress in the ground calculated by stability analysis is different at each point of the sliding surface. In such cases, and if the soil exhibits a strain softening behavior, it is thought to be rational to examine the stability of the ground using the residual strength if the shearing stress on the sliding surface exceeds the maximum shearing strength.

Also, in consolidated undrained triaxial test, there are cases where the maximum of deviatoric stress is different from that of stress ratio. It is said that the maximum of deviatoric stress coincides with the maximum of stress ratio if the specimen could be completely saturated by using back pressure, but there are some experimental reports denying this assertion, as shown in this report [1), 2), 3), 4), 5)] . In fact, it is found that after the deviatoric stress arrives at the maximum, it decreases afterwards while the stress ratio increases. This is called strain softening behavior [6), 7), 8)].

Adachi et al developed a modified Adachi-Oka's elasto plastic constitutive model which can describe not only strain-hardening-softening behavior but also dilatancy characteristics [9)]. Based on a new volumetric strain dependent potential function, this model exhibits a positive dilatancy in the post peak area of the undrained triaxial shearing test result for rock. In order to describe some aspects of the mechanical behavior of highly structured soils, Asaoka et al introduced the superloading yield surface concept to the original Cam Clay model. In the constitutive modeling, a new critical state parameter is adopted to give the watershed of the stress domain for hardening and softening [10)]. This model is capable of predicting softening below the critical state line with plastic volume compression. Hashiguchi et al formulated the elasto plastic constitutive equation based on the subloading yield surface concept [11), 12)]. This model can also predict the strain-hardening-softening behavior of soils. These three typical soil models which can describe

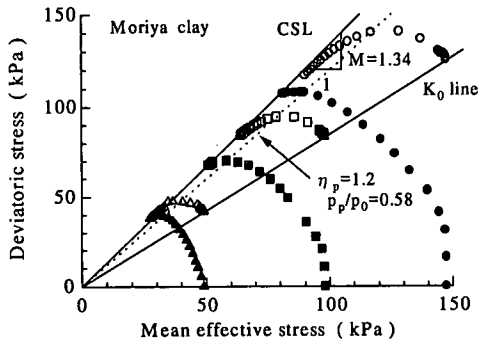

Fig.1 Observed undrained stress paths

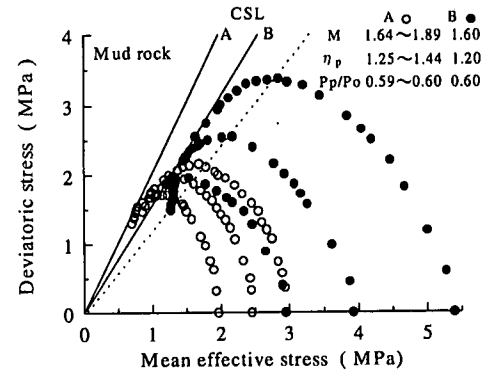

Fig.2 Observed undrained stress paths

Table 1 Physical properties of soil samples

	Gs	ω_n(%)	ω_L(%)	ω_P(%)	Grading(%) clay	silt	sand
Moriya clay	2.64	149.3	130.9	53.4	58.2	29.0	12.8
Mud rock A	2.18	119.6	172.7*	94.7*	$p_c \fallingdotseq$ 1.6 MPa		
Mud rock B	2.21	112.0			$p_c \fallingdotseq$ 2.3 MPa		

*grading < 420 μ m

the undrained softening behavior, adopt the associated flow rule and need several special soil constants. It is not easy to determine the soil constant by the conventional test.

Morio et al proposed an isotropic hardening elastoplastic constitutive model which can successfully simulate the strain softening behavior of extremely loose sand under undrained triaxial condition [13]. However, it is well known that unavoidable defects are involved in the non associated constitutive model when the model is applied to the boundary value problem [14]. Stability conditions of non symmetric rate type constitutive model are examined and compared qualitatively with the triaxial tests by Tobita [15]. Tobita showed a simple and convenient stability condition being accordance with the experimental observation and pointed out that the formulation with a non associated flow rule required a futher investigation from both theoretical and experimental standpoints. The stress strain relationship exhibiting the strain softening behavior is not elucidated yet.

In view of the importance of strain softening behavior as mentioned before, i.e. with decreasing deviatoric stress but increasing stress ratio, an elastoplastic constitutive soil model is presented which can predict the foregoing response in undrained triaxial test of normally consolidated soils.

The purpose of this paper is mainly to discuss the undrained behavior of normally consolidated clay and rock in relation to the yield function. From a practical view point, it can be considered to be important that the model does not need any special test in determining soil constants, except consolidated undrained triaxial test, and that it can simulate the strain softening behavior of triaxial test. The validity of the constitutive models is examined only by triaxial test results.

2. SAMPLES AND EXPERIMENTS

The alluvial clay samples were obtained from Moriya, Ibaraki, which is located in the alluvial low land along the Kokai River. The soft ground consists of a 0-7 m peat layer and a 7-14 m clay stratum. Undisturbed saturated normally consolidated clays were taken by foil sampling.

The diatomaceous mud rock of the late Tertiary Miocene Epoch accumulated in Suzu, Ishikawa is porous and of high water content, and is well known by its unique mechanical behavior [4]. Two kinds of mud rock specimens are obtained from different positions and different depths.

Because the clay sample under low overburden pressure of 15 kPa is extremely soft, and the mud rock sample is trimmed with a knife, both undisturbed samples may have considerable influence of disturbances while made into specimens.

The undrained shear test ($\overline{CU}$) is performed by the strain control method(strain rate of 0.1%/min). The specimens, 5cm diameter and 12cm high, with drain paper are consolidated under isotropic or K_o condition for 24 hours. During consolidation and shearing, back pressures of 98.1 kPa is applied to clay and 490.5 kPa is applied to mud rock and the volumetric strain time curves are measured to check

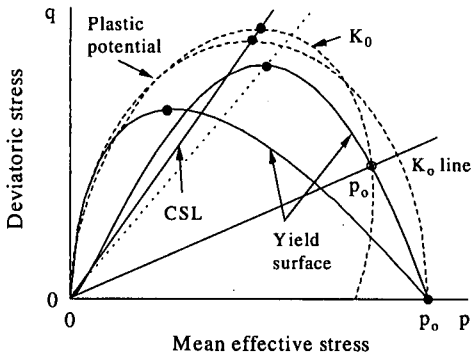

Fig.3 Plastic potential and yield function of Model 1

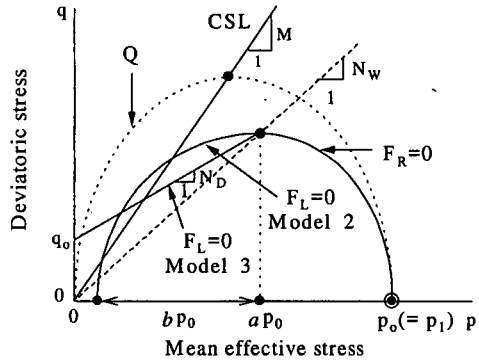

Fig.4 Yield function of Model 2 and 3

the End Of Primary consolidation. EOP of the both samples is below 200 minutes.

The physical properties of the sample are shown in **Table 1**.

3.TEST RESULTS AND DISCUSSION

Figures 1 and **2** show the undrained stress paths obtained from the consolidated undrained triaxial test using clay and mud rock, respectively. The clay samples were both isotropically and anisotropically consolidated. Strain softening behavior is observed with both clay and mud rock samples. For the isotropic consolidated clay sample, the deviatoric stress q in axisymmetric stress state finds its maximum at 60% of initial mean effective stress p_o (the prime which shows effective stress is omitted in this report), while stress ratio η =q/p increases afterwards and reaches the critical state. The dotted line in **Fig.1** shows the maximum deviatoric stress $q_P = \eta_P p_P$ at $\eta_P = 1.20$. Subscript p means the value of the peak deviatoric stress, while the maximum stress ratio at the critical state is M=1.34. As shown in **Fig.2**, the stress ratio η_P of mud rocks at the peak deviatoric stress is not kept constant. Further experimental investigations are needed to find the cause of this scattering.

The undisturbed clay or rock samples used for the experiment were very soft or hard, respectively, so that there is a possibility that the specimen had been considerably disturbed before the triaxial test. That may be the reason why the degree of the disturbance is large, and the axial strain, when the deviatoric stress is maximum, is 1-3% for clay and 3-4% for mud rock. Clear slip surface can be observed in all mud rock specimens after the shear test.

The degree of strain softening of the isotropically consolidated mud rock sample (**Fig.2**) is larger than that of the clay sample.

In determining the constants of the constitutive model mentioned in Chapter 4, η_P and p_P/p_0 values of consolidated undrained triaxial compression test are used. The p_P/p_0 of mud rock sample A is about 0.6, as well as of the clay sample, but that of mud rock sample B is 0.52.

4. STRAIN SOFTENING BEHAVIOR AND NON ASSOCIATED FLOW RULE

(1) Stress strain relation

The volumetric strain increment δv and shear strain increment $\delta \varepsilon$ of a soil element in triaxial loading, is the sum of an elastic and a plastic strain component, indicated by superscripts e and p, respectively, and expressed analytically by

$$\begin{bmatrix} \delta v(=\delta v^e + \delta v^p) \\ \delta \varepsilon(=\delta \varepsilon^e + \delta \varepsilon^p) \end{bmatrix} = \begin{bmatrix} C_{11} & C_{12} \\ C_{21} & C_{22} \end{bmatrix} \begin{bmatrix} \delta p \\ \delta q \end{bmatrix} \quad (1)$$

where δp is the mean effective stress increment, and δq is the deviatoric stress increment.

In the course of determining the coefficient C_{ij} of Eq.(1), a non associated flow rule is adopted in order to account for strain softening behavior. Specifically, considering a yield function F and a plastic potential Q, functions of q, p, the C_{ij} of Eq. (1) are given by

$$C_{11} = \frac{1}{H}\frac{\partial F}{\partial p}\frac{\partial Q}{\partial p} + \frac{1}{K}, \quad C_{12} = \frac{1}{H}\frac{\partial F}{\partial q}\frac{\partial Q}{\partial p}$$

$$C_{21} = \frac{1}{H}\frac{\partial F}{\partial p}\frac{\partial Q}{\partial q}, \quad C_{22} = \frac{1}{H}\frac{\partial F}{\partial q}\frac{\partial Q}{\partial q} + \frac{1}{3G} \quad (2)$$

where H is the hardening plastic modulus, K is the elastic bulk modulus, G is the elastic shear modulus. Those three moduli are given by

$$H = -\frac{\partial F}{\partial p_0}\frac{\partial p_0}{\partial v^p}\frac{\partial Q}{\partial p} \quad (3)$$

$$K = \frac{1+e_0}{\kappa} p \tag{4}$$

$$G = \frac{3(1-2\nu)}{2(1+\nu)} K \tag{5}$$

where p_0 is a size parameter of the yield surface corresponding to initial void ratio e_0, ν is Poisson's ratio, and κ is the swelling index.

The plastic potential Q consists of a rotated and distorted ellipse, shown by a dotted line in **Fig.3**, which becomes identical to the potential of the Modified Cam Clay model for isotropic consolidation. The degree of rotation and distortion depends on the degree of anisotropy, and is measured by an anisotropic variable α which enters the analytical expression proposed by Dafalias [16), 17)].

$$Q = q^2 + 2\alpha pq + \alpha^2 pp_0 + M^2 p(p - p_0) \tag{6}$$

$$\alpha = \frac{\eta_k^2 + 3(1-\kappa/\lambda)\eta_k - M^2}{3(1-\kappa/\lambda)} \tag{7}$$

$$\eta_k = 3(1-K_0)/(1+2K_0) \tag{8}$$

where M is the slope of the critical state line.

The anisotropic variable α is equal to zero for isotropically consolidated sample, while for one dimension consolidated sample, α is calculated in closed form by the coefficient of earth pressure at rest K_0 [16), 17)]. The anisotropic variable α is introduced in the plastic potential, in order to bring the stress strain relationship of K_0 consolidated soil close to experimentally observed values.

For the yield function three models will be considered for comparison, all associated with the same plastic potential of Eq.(6). The yield function of Model 1 is analytically expressed by

$$F = q - mp^n \log_e (p_0/p) = 0 \tag{9}$$

where m and n are constants and the corresponding yield surface is shown in **Fig.3** by a solid line.

If m=M and n=1, Eq.(9) agrees with the yield function of Original Cam Clay model [18), 19)]. Depending on the values of m and n, the top point of the yield surface may be located to the left or the right of the CSL, inducing strain hardening or strain softening response, respectively.

The yield surfaces of Model 2 and 3 for isotropically consolidated soil are shown in **Fig.4** by solid lines.

The yield surface is identical for both models when $p \geqq ap_0$. Its shape is elliptical and lies to the right of a stress ratio value $\eta = q/p = N_W$, given analytically by

$$F_R = (1-a)^2 q^2 + a^2 N_w^2 ((p - ap_0)^2 - p_0^2(1-a)^2) = 0 \tag{10}$$

Table 2 Soil parameters used for the Models

Model	Model 1	Model 2	Model 3
Constants	m, n	N_W, a, b	N_W, N_D, a, q_0

For $p < ap_0$, the yield surface of Model 2 is also elliptical and lies to the left of $\eta = N_W$, given analytically by

$$F_L = b^2 q^2 + a^2 N_W^2 (p - ap_0)^2 - a^2 b^2 N_W^2 p_0^2 = 0 \tag{11}$$

Finally, the yield surface of Model 3 to the left of $\eta = N_W$ is a straight line with equation

$$F_L = q - N_D p - q_0 = 0 \tag{12}$$

where a, b, N_W, N_D and q_0 are constants controlling the shape of yield surfaces, and $N_D = N_W - (q_0/ap_0)$ in order to have the line of Eq.(12) passing through the same point on $\eta = N_W$ as that of Eq. (11).

The case where the constants are a=b=1/2 and N_W=M in equations (10) and (11), and α=0 in Eq. (6), corresponds to that of an associated flow rule with the yield surface and plastic potential identical to Modified Cam Clay model. The corresponding stress strain relationship will be of the strain hardening type.

This paper is mainly concerned with the simulation of stress softening behavior using a non associated flow rule for saturated normally consolidated soil, under the undrained shearing, during which the deviatoric stress reaches a maximum q_P and subsequently diminishes while the stress ratio becomes maximum η_{max} (=M), i.e. at critical state.

Soil constants λ, κ, M, ν and K_0 are needed in common with these three models. Another constants are shown in **Table 2**. Constants m and n in Model 1 are determined by the peak deviatoric stress of the undrained stress path as shown in Chapter 5.

Also N_W, N_D, a, b and q_0 depend on the observed undrained stress path but it is difficult to determine quantitatively.

(2) Strain softening behavior of the models

Fig.5 through **Fig.8** show examples of calculated effective stress paths and deviatoric stress axial strain relation in undrained triaxial test for isotropically and K_0 consolidated soils, by the strain softening type elastoplastic constitutive models presented in the foregoing.

The constants used for the calculation are shown in the figures. Though strain softening behavior is calculated both in isotropic and K_0 consolidated

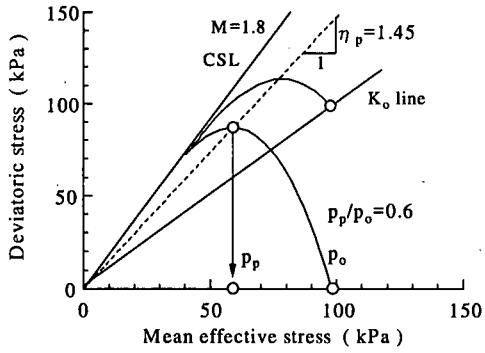

Fig.5 Calculated undrained stress paths of Model 1

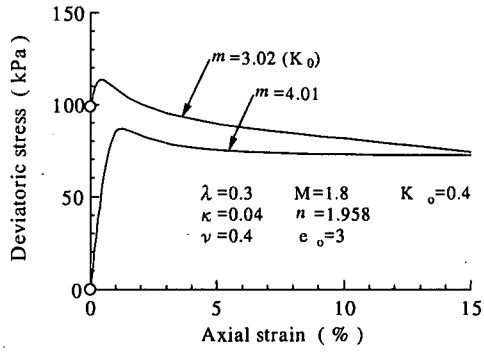

Fig.6 Calculated stress strain relations of Model 1

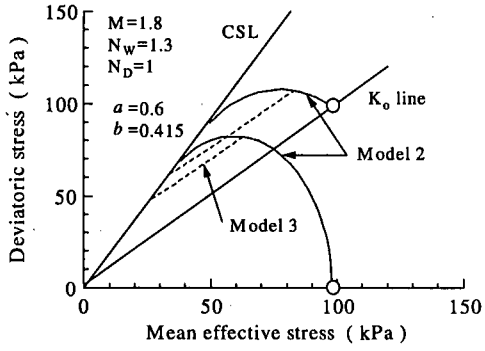

Fig.7 Calculated undrained stress paths for Model 2 and 3

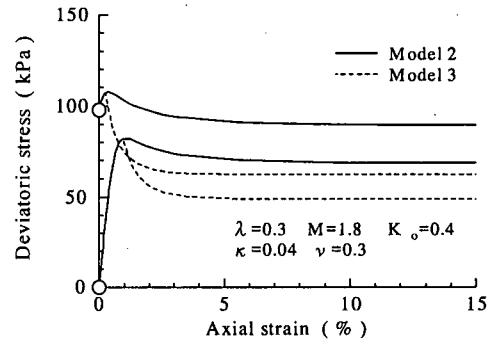

Fig.8 Calculated stress strain relations for Model 2 and 3

soil, the degree of strain softening of Model 1 and 2 is not so large. It is possible to simulate extremely large strain softening behavior, using a small yield surface that does not cross the critical state line CSL. On the contrary, the degree of strain softening by Model 3 shown with a dotted line in **Fig.7** and **Fig.8** is large. If the slope N_D of yield surface F_L in Eq. (12) is increased, simulation of large strain softening behavior is possible. However, as is shown in **Fig.7**, the behavior of effective stress path becomes unnatural and different from what it actually is, with its sudden straight-line change at the beginning of the softening process.

Furthermore, if the shape of yield surface is drastically changed in order to control the degree of strain softening, it will not define realistically the range of elastic behavior of soil. These qualitative assertions define the problems and limitations of the constitutive models presented in this report.

5. SIMULATION OF UNDRAINED TRIAXIAL TEST

(1) Determination of soil constants

The differential equation of the effective stress path in undrained shear test is obtained by setting the total volumetric strain increment δv in Eq.(1) equal to zero. This differential equation can then easily be integrated to yield the undrained stress path expression for Model 1 [17].

$$q = \frac{\lambda}{\lambda - \kappa} m p^n \log_e (p_0 / p) \qquad (13)$$

where λ is the compression index.

Eq.(13) can be used to specify model constants m and n from the experimentally measured values of p_p,q_p and $\eta_p = q_p / p_p$ at the peak of the undrained stress path. It suffices to set dq/dp=0, which together with Eq. (13) at q_p, p_p is solved to yield

Table 3 Soil parameters used for the calculation

	λ	κ	e_0*)	ν	K_0	M
Moriya clay	0.754	0.094	2.840	0.3	0.46	1.34
Mud rock A	0.642	0.071	2.700	0.3		1.64~1.89
Mud rock B	0.951	0.105	2.295	0.3		1.60

*) void ratio at isotropic consolidated pressure,
Moriya clay 98.1kPa, mud rock 1.47(A), 2.45(B) MPa

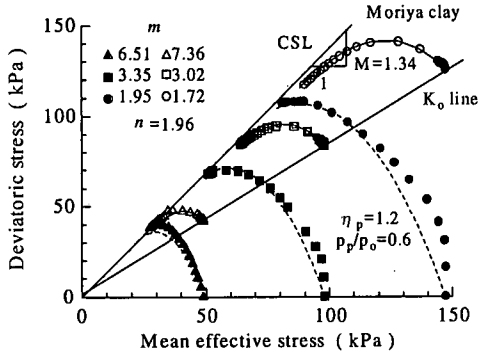

Fig.9 Observed and calculated undrained stress paths of Model 1

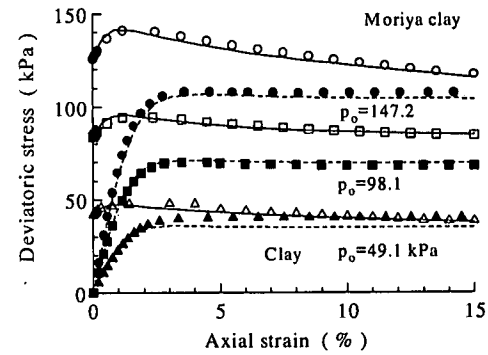

Fig.10 Observed and calculated stress strain relations of Model 1

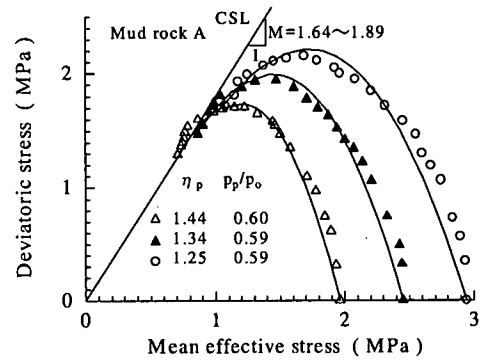

Fig.11 Observed and calculated undrained stress paths of Model 1

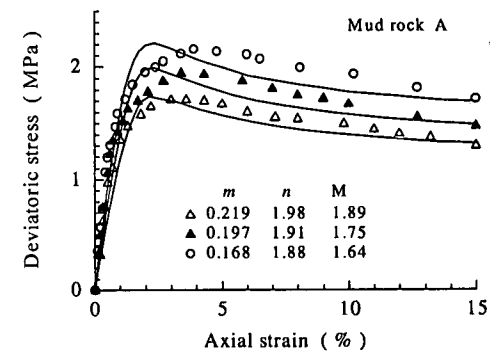

Fig.12 Observed and calculated stress strain relations of Model 1

$$m=n(1-\kappa/\lambda)\eta_p/p_p^{n-1},\quad n=1/\log_e(p_0/p_p) \qquad (14)$$

Soil constants that are necessary for simulation of consolidated undrained triaxial tests, some of which were derived from results of consolidation tests, are shown in **Table 3**. The Poisson's ratio ν is assumed to have the values shown in **Table 3**.

(2) Simulative capability of the model

The calculated undrained stress paths and deviatoric stress versus axial strain curves by Model 1 are shown in **Fig.9** and **Fig.10** for clay sample, in **Fig.11** and **Fig.12** for mud rock sample A, and in **Fig.13** and **Fig.14** for mud rock sample B. In the clay sample, some deviation from experimental data of the isotropically consolidated sample is observed, but the simulation results agree in general fairly well with test results.

The calculated undrained paths of mud rock sample A agree well with test results, but the deviation of calculated stress strain curve is large. In particular the maximum calculated deviatoric stress is reached at axial strain 2% or less, while the observed value of axial strain is as large as 3-4%. For the mud rock sample B, the calculated effective stress path is close to the observed one, but again a deviation from the data is observed for stress strain curve, which, nevertheless, is quite smaller than the one observed for mud rock sample A. For example, the result in **Fig.14** shows that the axial stress reaches its maximum value around 4% strain, and this is in agreement with data. It can be considered that the deviation of the calculated axial strain at the maximum deviatoric stress is influenced by the observed value of η_p. On the figures the experimentally determined values of η_p and p_p/p_o are referred, based on which the values of m and n are calculated from Eq.(14). Different sets of m and n values are used in the simulations. If one set of m and n values is used for each sample, taken as the average of the different sets, the simulation of the data will be less successful, but still within an acceptable range of deviation.

For Models 2 and 3, a straightforward approach to determine the constants as in the case of Model 1 via Eq.(14), has not been derived yet. If constant a

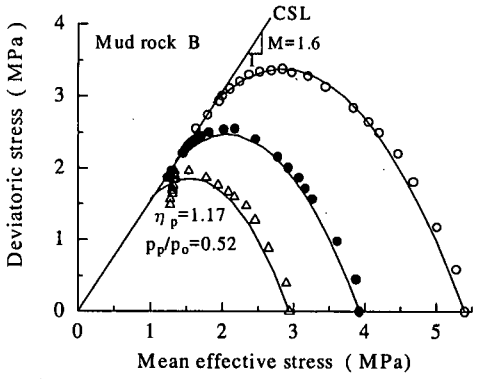

Fig.13 Observed and calculated undrained stress paths of Model 1

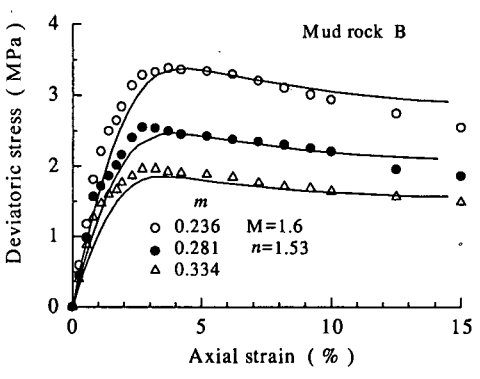

Fig.14 Observed and calculated stress strain relations of Model 1

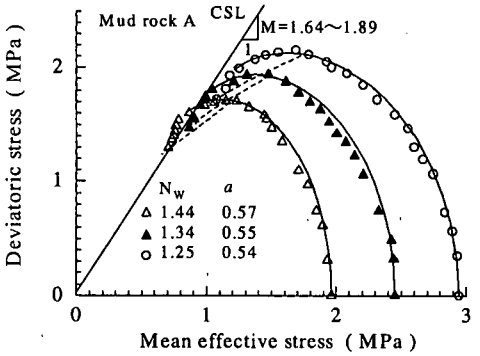

Fig.15 Observed and calculated undrained stress paths of Model 2 and 3

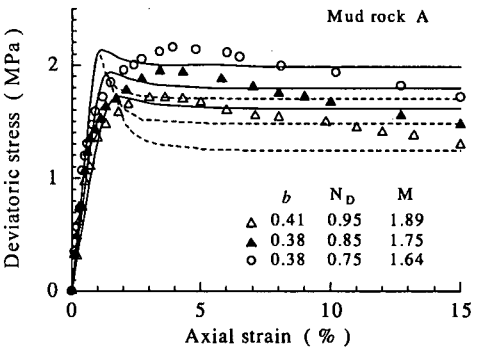

Fig.16 Observed and calculated stress strain relations of Model 2 and 3

of Eq.(10) for F_R is made equal to p_p/p_o, the deviatoric stress will be found larger than actually observed, which is known from the comparison of the yield function and Eq.(13) of effective stress path. Therefore, it was assumed that N_w is equal to η_p and the constant a was set a little smaller in order to make the calculated maximum deviatoric stress to agree with the observed one. In order to describe the large strain softening behavior, constant b was determined by the point where the ellipse F_L touches the CSL. Also, constant N_D was decided on the condition that the residual strength agrees with observed value. The calculated results of effective stress path and deviatoric stress axial strain curve are shown by solid lines in **Fig.15** and **Fig.16**, as well as the observed ones by discrete symbols.

The calculated results by Model 2 and 3 are identical till strain softening occurs, because F_R is the same for both models. The solid line in **Fig.15** and **Fig.16** refers to Model 2, while the dotted line to Model 3. Because both models adopt an oval shaped yield surface F_R, the axial strain at the maximum deviatoric stress is smaller than Model 1, and the gap with observed axial strain increases. Furthermore, because of the different F_L, Model 2 cannot simulate large strain softening behavior. Model 3 cannot reproduce realistic strain softening behavior till it reaches residual strength even if residual strength is made equal to observed one.

6. CONCLUDING REMARKS

The paper presents three elastoplasic constitutive soil models exhibiting strain softening behavior and evaluates simulative capability of the proposed model using the undrained triaxial test results of normally consolidated soils. It has been demonstrated that the calculated results of models using a non associated flow rule agree well with observed ones, if the degree of strain softening is small. Key to successful simulation is the use of anisotropic plastic potential for the case of one dimensional consolidation before undrained shear.

Among the three kinds of yield functions, the strain softening behavior of Model 1, is based on the transformed yield function of Original Cam Clay, and yields the nearest to actual experiment results. Also, material constants contained in the constituti-

ve equation are easy to decide from the experiment, which makes the equation practical. Because the models put great importance only to strain softening behavior of normally consolidated soil under undrained conditions, examination of the overconsolidated soil and softening behavior under drained conditions are works to be pursued in the future.

ACKNOWLEDGMENT : Y.F. Dafalias would like to acknowledge partial support of his contribution by the NSF grant CMS-9800330.

REFERENCES

1) Bjerrum, L. Simons, N. and Torblaa, I. : The effect of time on the shear strength of a soft marine clay, Proc. of Earth Pressure Prob., Vol.1, pp.148, 1958.
2) Akai, K. and Kotani, A. : The Effect of Back Pressure on Consolidation and Shearing of Undisturbed Saturated Clay, Proc. of JSCE, No.91, pp.1-7, 1963. (in Japanese)
3) Liao, H.J., Akaishi, M. and Hayashi, M. : Residual Strength Characteristics of Discontinuous Diatomaceous Soft Rock, Proc. of JSCE, No.529, pp.103-111, 1995. (in Japanese)
4) Maekawa, H. and Miyakita, K. : Mechanical Properties of Diatomaceous Soft Rock, Proc. of JSCE, No.334, pp.135-143, 1983. (in Japanese)
5) Nishi, K., Okamoto, T. and Esashi, H. : Strength Deformation Characteristics of Mud Stone under Some kinds of Loading Conditions and its Unificative Interpretation, Proc. of JSCE, No.338, pp.149-158, 1983. (in Japanese)
6) Adachi, T. and Oka, F. : Strain Softening Plasiticity Constitutive Equation of Mud Rock, Proc. of JSCE, No.445, pp.9--15, 1992. (in Japanese)
7) Lo, K. Y. and Lee, C.F. : Stress analysis and slope stability in strain-softening materials, Geotechnique, Vol.23, No.1, pp1-11, 1973.
8) Dounias, G.T., Potts, D.M. and Vaughan, P.R. : Finite Element Analysis of Progressive Failure: Two Case Studies, Computers and Geotechnics, Vol.6, pp155-175, 1988.
9) Adachi, T., Oka, F., Koike, A. and Koike, M. : Modified Adachi-Oka's elasto plastic constitutive model for soft rock, Proc. of JSCE, No.559, pp.31-40, 1998. (in Japanese)
10) Asaoka, A., Nakano, M., and Noda, T. : Superloading yield surface concept for highly structured soil behavior, Soils and Foundations, Vol.40, No.2, pp.99-110, 2000.
11) Hashiguchi, K. and Okayasu, T. : Time-dependent elastoplastic constitutive equation based on the subloading surface model and its application to soils, Soils and Foundations, Vol.40, No.4, pp.19-36, 2000.
12) Hashiguchi, K., Ueno, M. and Chen, Z.P. : Elastoplastic constitutive equation of soils based on the concepts of subloading surface and rotational hardening, Proc. of JSCE, No.547, pp.127-144, 1996. (in Japanese)
13) Morio, S., Kusakabe, S., Yasufuku, N. and Hyodo, M. : Analytical Investigation of Instability for Saturated Sand under Triaxial Condition, Proc. of JSCE, No.499, pp.157-165, 1994. (in Japanese)
14) Runesson, K., Axelsson K. and Klinski M. : Characterisitics of Constitutive Relations in Soil Plasticity for Undrained Behavior, *Int. J. Solids and Structures*, Vol.29(3), pp.363-380, 1992.
15) Tobita, Y. : Stability Condition of Non-symmetric Rate Type Constitutive Model, Journal of Structural Engineering, JSCE, Vol.42(A), pp.297-306, 1996. (in Japanese)
16) Dafalias, Y.F. : An anisotropic critical state soil plasticity model, Mechanics Research Communications, Vol.13(6), pp.341-347, 1986.
17) Dafalias, Y.F. : An anisotropic critical state clay plasticity model, Proc. of 2nd International Conference on Constitutive Law for Engineering Materials, Vol.1, pp.513-521, 1987.
18) Roscoe, K.H., Schofield, A.N. and Thurairajah, A. : Yielding of clay in state wetter than critical, Geotechnique, Vol.13, No.3, pp.211-240, 1963.
19) Atkinson, J.H. : *Foundations and Slopes*, McGraw-Hill Book Company (U.K.) Limited, 1981.

(Received April 19, 2000)

正規圧密粘土と泥岩の非排水ひずみ軟化挙動

山田道男・赤石勝・Yannis F. DAFALIAS

非関連流動則を用いて正規圧密粘土ならびに泥岩の非排水ひずみ軟化挙動に関する弾塑性構成モデルを提案した．提案した３つの降伏関数でモデルの適用性と限界を検討した．ひずみ軟化挙動の再現計算結果は，沖積粘土と珪藻質泥岩の非排水三軸圧縮試験結果と比較した．提案したモデルの１つは，小さなひずみ軟化挙動を考慮した非排水応力ひずみ関係として適用しうる．